IMAGING THE INTERACTION OF MULTIBEAM/MULTIMODE ULTRASONIC TRANSDUCERS WITH MANUFACTURING AND SERVICE-INDUCED FLAWS

George Gruber and Dennis Hamlin

Southwest Research Institute
6220 Culebra Road,
San Antonio, Texas 78284

INTRODUCTION

Type, through-wall dimension (depth), and location are the most important flaw characteristics that need to be determined for the fracture-mechanics evaluation of a flawed component or part. In this paper, the three-step approach to the ultrasonic evaluation of flawed reactor pressure vessel components (i.e., flaw detection, identification, and sizing) are discussed in relation to fatigue cracks, slag inclusions, incomplete fusion flaws, and porosity clusters. The emphasis is on flaw identification (cracks vs. benign flaws) which must take place before estimating the depth of the flaw. The composite pulse patterns obtained with four multibeam/multimode SLIC transducers [1] for two model flaws (a side-milled notch and a side-drilled hole) and two real flaws (fatigue crack and slag inclusion) are imaged in a B-scan format.

Each image contains up to three readily recognizable and interpretable slanted lines formed by plotting the time-of-flight or screen position (P_i) for the main and satellite pulses (i=1, 2, or 3) along the -Y axis against transducer position X along the X axis. The amplitude-modulated $P_i(X)$ lines thus constitute permanent records of the flaw-type-and-size-information-carrying satellite pulses as they move across the instrument screen during automatic scanning of the flaw with a SLIC transducer. The theoretical foundations of the crack-imaging concepts are given in the companion paper [1]. The color-graphic displays of the P_i vs. X and A_i (pulse amplitude) vs. X data acquired during remote transducer scanning with a four-channel Enhanced Data Acquisition System (EDAS) instrument [2] made it possible for the traditionally trained ultrasonic examiners to fully characterize a material discontinuity in near real time. In most cases, the black-and-white images of the type included in this paper are adequate for the interpretation of the PX data in terms of flaw type, size, and location.

THE PROBLEM

The principal limitation to detection (and, more so, to characterization as to type and size) of near-surface flaws in cladded reactor

pressure vessels is the nonrelevant indications originating at the clad-to-base metal interface. These indications mask not only the weak satellite pulses diffracted/scattered by the extremities of a planar/volumetric flaw, but also the reflected pulse used to detect the flaw in the first place. Manual ultrasonic examiners often have difficulties in interpreting in real time the wiggly lines in motion on the instrument screen in terms of flaw type and depth. Early attempts to develop indication screening criteria (relevant vs. nonrelevant or "signal" vs. "noise") and flaw identification procedures were generally hampered by being based on restricted (single-channel) data sets, and being limited to pulse-pattern (echo structure and dynamics) information derived from single A-scan ("snapshot") traces.

APPROACH AND OBJECTIVES

Our current approach to proceduralizing parts of the serial flaw identification and sizing tasks is based on the availability of the Multibeam Inspection Technology[sm] software and hardware items listed in Table 1. The amplitude-based and time-of-flight ultrasonic techniques recommended for full flaw characterization are discussed elsewhere [3-4]. The SLIC-40/50/30 transducers are discussed along with a computer modeling capability in the companion paper [1]. The data acquisition and imaging system is described in ref. 2. The objectives of this paper are to disclose the recently developed ultrasonic indication and analysis guidelines and present the characteristic images (ultrasonic "fingerprints") obtained for four flaws.

Table 1

BUILDING BLOCKS OF MULTIBEAM INSPECTION TECHNOLOGY

	Software		Hardware
(1)	Time-of-flight and amplitude-based techniques which lead to reliable flaw detection and identification and accurate estimation of flaw location, size, and orientation.	(1)	Multibeam/multimode (SLIC) transducers which provide more A-scan information about the detected flaw than an examiner can use in real time.
(3)	A computer modeling capability for the SLIC transducers which permits comparison of the measured variations in pulse flight time (T) or position (P) and amplitude (A) with transducer position (X) with the PAX plots computed for a series of planar flaws with known characteristics.	(4)	A four-channel doublet acquisition and imaging system (EDAS) which automatically displays, in near real time, all of the pulse amplitude and flight time data acquired during transducer scanning in a B-scan format.
(5)	Flaw diagnostic signs which lead to reliable flaw identification (cracks vs. slags, porosity cluster, and incomplete fusion flaws).	(6)	An expert system which automatically recognizes the diagnostic signs of known flaw types in the images of a detected flaw.

INDICATION CLASSIFICATION AND FLAW IDENTIFICATION GUIDELINES

Table 2 contains a listing of indication screening criteria and flaw diagnostic signs developed around the SLIC transducers described in Table 3. The intent is to exploit the seven most reliable and informative Table 2 indication properties and the Table 3 multibeam/ multimode transducers to distinguish between cracks and other flaws with 95 percent or higher levels of confidence. The impetus for the development of flaw identification procedures is the readily observable differences and similarities in the ultrasonic fingerprints of the cracks, slag inclusions, incomplete fusion flaws, and porosity clusters.

FINGERPRINTING OF FOUR FLAWS

To demonstrate the usefulness of the SLIC transducers in full flaw characterization, the Table 3 transducers were connected to a four-channel EDAS [1]; and the stacked A-scans obtained for a side-milled notch, side-drilled hole, fatigue crack, and slag inclusion from the +X scan direction were imaged. The resulting color flaw fingerprints are reproduced in black-and-white in Figs. 1 and 2.

Proper indication classification as to its relevancy and proper indication analysis as to its seven properties lead to reliable flaw identification. For example, if the echo structure obtained with the SLIC-40 (Channel I) appears to be "complex and discontinuous" with both transverse (X) and lateral (Y) scanning, then the source of the indication is likely to be a slag, particularly if the echo is "strong" and "highly persistent" with transducer skewing. By the same token, if the Channel I echo structure is "composite," the satellite pulse (pulse 2) is "weak," the envelope of the main pulse (pulse 1) is "narrow and

Table 2

INDICATION SCREENING CRITERIA AND FLAW DIAGNOSTIC SIGNS

Indication Property	Definition	Diagnostic Signs
Echo strength	Maximum pulse amplitude	• Weak (crack) • Strong (porosity, incomplete fusion, slag)
Echo structure (A-scan)	Variation of pulse amplitude with time at a fixed transducer position (temporal energy distribution)	• Simple, smooth, and continuous (incomplete fusion) • Composite (crack, porosity) • Complex and discontinuous (slag)
Echo envelope	Variation of the amplitude of a single pulse with transducer position (spatial energy distribution)	• Narrow and symmetric (porosity, crack) • Broad and asymmetric (incomplete fusion)

Table 2 (Cont'd)

INDICATION SCREENING CRITERIA AND FLAW DIAGNOSTIC SIGNS

Indication Property	Definition	Diagnostic Signs
Echo dynamics	Comparison of the echo envelopes for the two or three pulses constituting a composite echo structure	• Synchronous (porosity) • Asynchronous (crack)
Echo persistence	Rate of pulse amplitude change with transducer skewing	• Low (crack, incomplete fusion) • High (porosity, slag)
Echo image (B-scan)	Variation of color-modulated pulse amplitude and pulse position with transducer position	• Crack-like • Slag-like • Incomplete-fusion-like • Porosity-like
Phase distribution	Comparison of the phases (0° or 180°) of the pulses constituting a composite echo structure	• Phase reversal (crack) • No phase reversal (porosity)

Table 3

FUNCTIONAL DESCRIPTION OF A FOUR-CHANNEL ULTRASONIC DATA ACQUISITION AND IMAGING SYSTEM

CHANNEL 1: SLIC-40
Flaw Detection Channel

The multibeam transducer of this instrument channel yields high signal-to-noise ratio for reliable flaw detection and accurate estimation of flaw length.

CHANNEL II: SLIC-45
Flaw Identification Channel

The multimode transducer of this instrument channel yields high signal-to-noise ratio and characteristic satellite-pulse patterns for reliable flaw identification (crack vs. other flaw types) and crack detection or confirmation.

CHANNEL III: SLIC-30
Flaw Characterization Channel

The multibeam transducer of this instrument channel yields characteristic satellite-pulse patterns for reliable flaw identification and accurate estimation of flaw location, orientation, depth, and shape.

CHANNEL IV: SLIC-50
Flaw Characterization Channel

The multimode transducer of this instrument channel also yields characteristic satellite-pulse patterns for reliable flaw identification and accurate estimation of flaw location, orientation, depth, and shape.

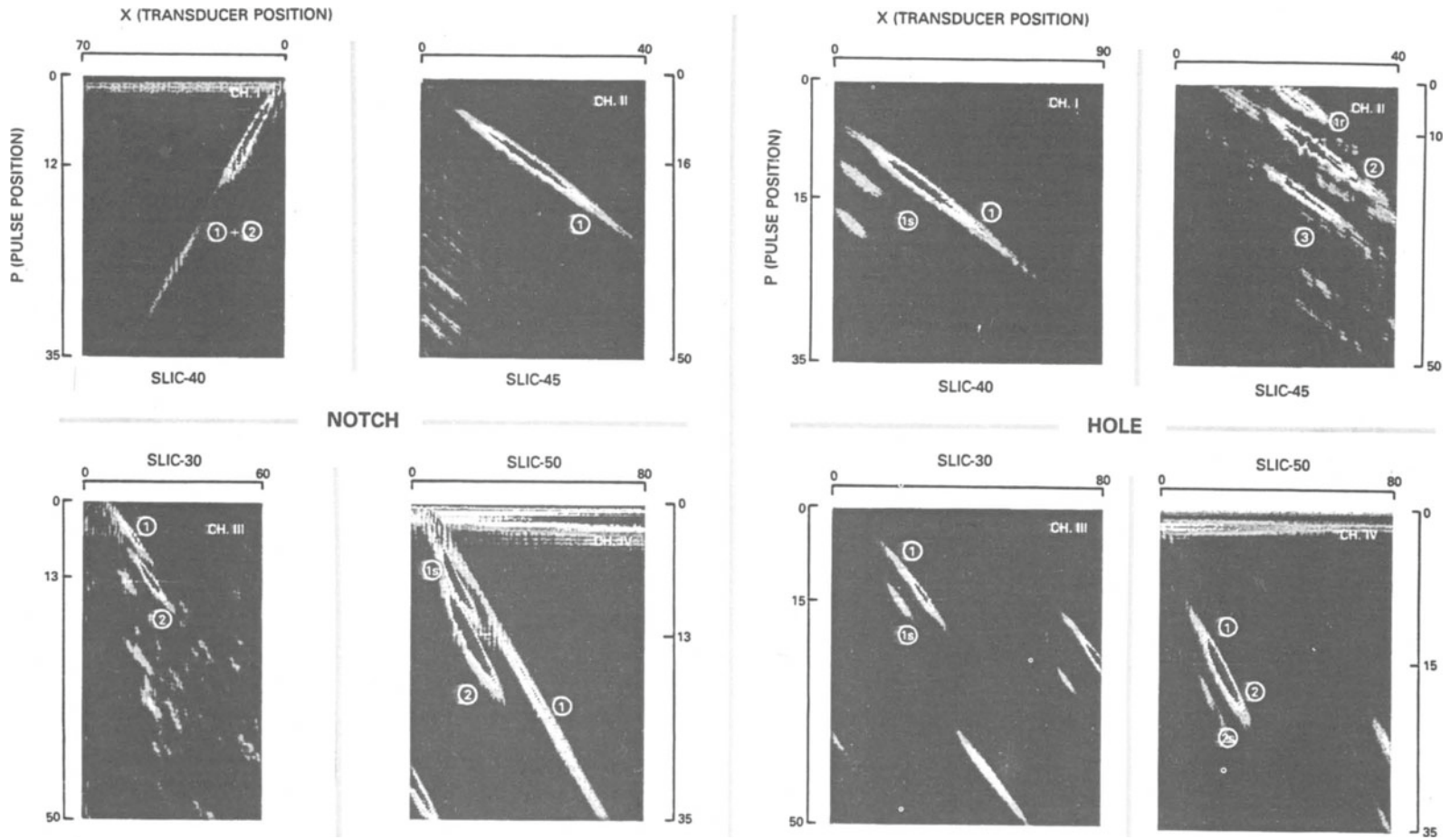

Fig. 1. Notch vs. hole diagnosis through fingerprinting

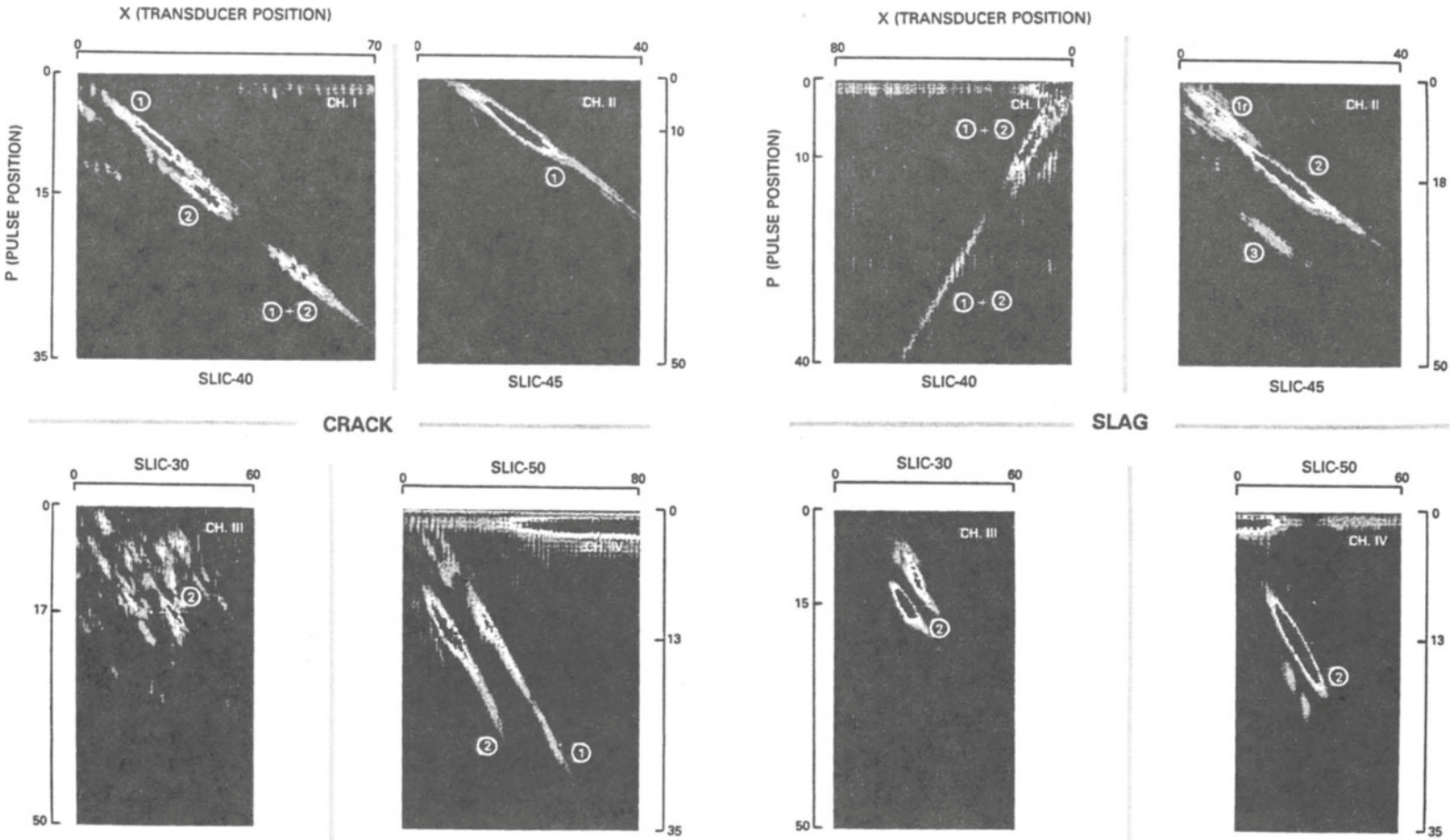

Fig. 2. Crack vs. slag diagnosis through fingerprinting

symmetric," the echo dynamic pattern is "asymmetric," the echo persistence is "low," and "phased reversal" is observed between the associated pulses, then the source of the indication is likely to be a crack. In agreement with model predictions [1, 5], slags (right side of Fig. 2) exhibit a hole-like fingerprint (right side of Fig. 1), and cracks (left side of Fig. 2) exhibit a notch-like fingerprint (left side of Fig. 1). Incomplete fusion flaws and porosity clusters have their own characteristic sets of ultrasonic fingerprints.

CONCLUSIONS

As a result of the described hardware and software developments, it has been shown that both the temporal (A-scan) and spatial (B-scan) distributions of the ultrasonic energy returning to a set of four transmit-receive transducers from a flaw of interest can be automatically recorded and permanently imaged for near real-time as well as later analyses.

REFERENCES

1. G. J. Gruber and T. A. Mueller, "Modeling the Interaction of Multibeam/Multimode Transducers with Fatigue Cracks in Cladded Reactor Pressure Vessels," in Review of Progress in Quantitative Nondestructive Evaluation, Vol. 8, 1989.

2. K. S. Pickens et al., "Techniques for Reduction and Analysis of Large UT Data Sets," in Review of Progress in Quantitative Nondestructive Evaluation, Vol. 7, pp. 839-846, 1988.

3. G. J. Gruber, G. J. Hendrix, and W. R. Schick, Materials Evaluation, Vol. 42, pp. 426-432, 1984.

4. G. J. Gruber, Int. J. Pressure Vessels and Piping, Vol. 22, pp. 225-232, 1986.

5. G. J. Gruber, J. Nondestructive Evaluation, Vol. 1, pp. 263-276, 1980.